Argon assimilation during thermal quench and runaway electron generation

G. Pautasso[1], M. Bernert[1], M. Dibon[1], M. Dunne[1], R. Dux[1], E. Fable[1], O. Linder[1],
P. McCarthy[2], A. Mlynek[1], G. Papp[1], the ASDEX Upgrade team[1] and the EUROfusion MST1 team[3]

[1] Max-Plank-Institute für Plasma Physik, D-85748, Garching, Germany
[2] Department of Physics, University College Cork, Cork, Ireland
[3] see author list in H. Meyer et al 2017 Nucl. Fusion 102014

1. Introduction

Fusion reactors of the tokamak type must rely on a large plasma current, an elongated plasma and a large major radius for a good confinement and a large fusion energy gain at affordable costs. Unfortunately, tokamak plasmas are subject to disruptions caused by MHD instabilities. Moreover, disruptions at reactor-relevant currents are predicted to convert a large fraction of the current into runaway electrons (REs) because of the large avalanche gain [1]. When quickly lost by the plasma (because the beam becomes MHD unstable) and deposited on the plasma facing components, the REs can cause serious damages (melting).

Well diagnosed experiments on existing tokamaks are indispensable for the benchmark of RE generation and suppression models, which can then be used for the simulation of reactor scenarios. Particularly the quest for RE loss mechanisms during both the thermal quench (TQ) and the RE beam lifetime, and for ways to enhance the losses are being pursued. In this spirit, RE experiments have been carried out "bona fide" in ASDEX Upgrade (AUG) since 2014 [2]. RE beams do not occur in AUG mitigated or unmitigated disruptions and they have to be generated in an unusual, otherwise uninteresting plasma scenario: Argon injection is used to induce a fast current quench (CQ) and consequent large toroidal electric field, a low density target plasma is chosen to minimize the friction force on the electrons, and a circular poloidal cross section is necessary in order to provide a vertically stable plasma.

This contribution is focused on the comparison of the measured RE current generated during the induced CQ with the current calculated with a zero dimensional (0-D) model (not discussed in [2]).

2. RE generation: experimental scenario

REs have been generated in AUG by injecting between 4.5×10^{20} and 4.8×10^{21} atoms of argon into low density circular target plasmas. Larger quantities of argon would induce a short lived RE beam, uninteresting for the purpose of our studies. Whether smaller quantities of argon or the use of neon would still induce a significant RE beam has not been tested yet. Argon was injected with one (sector 13) of the fast in-vessel valves available on AUG for disruption mitigation studies. The target plasmas had a toroidal current $I_p = 0.7 - 0.8$ MA, a low density (line averaged $n_e = 2 - 4\times10^{19}$ m^{-3}), a toroidal magnetic field of 2.5 T and 2 MW of ECRH power. The plasma equilibrium was kept constant. Experiments with different values of magnetic field, ECRH power and therefore electron temperature (T_e) were partially carried out but are not discussed here. Discharges with RMPs were discussed in [3] and, unless specified otherwise, they are excluded in the following analysis.

The injected argon induces a fast I_p decay, followed by a long-lived RE beam, carrying a toroidal current of up to 420 kA, and lasting up to half a second. Although the target plasmas were similar (repeats), different initial RE current (I_{RE}) values were observed, independently of the amount of argon injected and of other measurable plasma parameters. The "initial I_{RE}" is defined as the current at 10 ms after the arrival of the injected impurities at the plasma edge. A 0-D model is used in section 4 to discuss the parametric dependencies expected from theory versus those deduced from the experimental

measurements.

3. Electron density and argon assimilation

The assimilation of large quantities of argon injected in AUG has not been documented in the literature so far and therefore it is discussed here. The amounts of argon injected (N_{inj}) to create the RE beam are relatively small - compared to the amounts needed to reach the critical density - since larger quantities would suppress its generation. The corresponding fueling efficiency, $F_{eff} = \Delta n_{e,V\text{-}1}/ (N_{inj} /V_p) = 50$ +/- 15 % (fig. 1 *left*) is relatively large. $\Delta n_{e,V\text{-}1}$ is the increase of the electron density, averaged along the V-1 chord of the CO_2 interferometer during the 5 ms following the TQ (which occurs at t = 1.0055 s in fig. 1 centre). Measurements along the more-peripheral V-2 chord often indicate a density on the high field side different from the core density (fig. 1 *left,* probably because of gas influx from the inner wall during the TQ) and they are not used in this analysis. The magnetic equilibrium was available for all the discharges in fig. 1, e.g. the interferometer chord length crossing the plasma and the plasma volume (V_p) are known. The assimilated argon amount, $n_{Ar} = \Delta n_e / Z_{Ar}$, can then be evaluated when the average argon ion charge, Z_{Ar}, is known (see section 4).
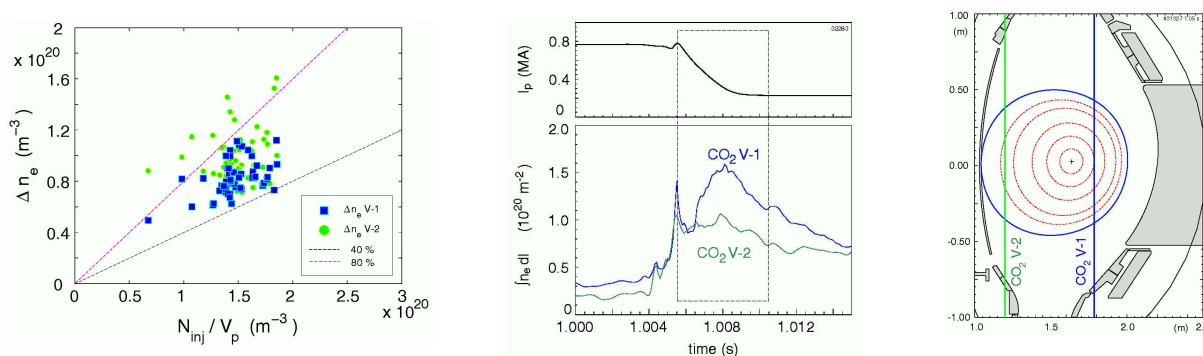

Figure 1. Left: increase of the plasma electron density versus the number of injected argon atoms per plasma volume. Discharges with RMP coils on are included. Centre: time traces of plasma current and line integrated density during the fast current quench. Right: CO_2 interferometer geometry.

4. RE generation: observations and comparison with theory

The generation of REs by argon injection in circular low density AUG plasmas has been reliably attained. Nevertheless the amount of I_{RE} generated is not always reproducible although the target plasmas are very similar. Moreover, RE generation is expected to depend on the electron and impurity densities but these dependencies do not immediately result from the experimental measurements.
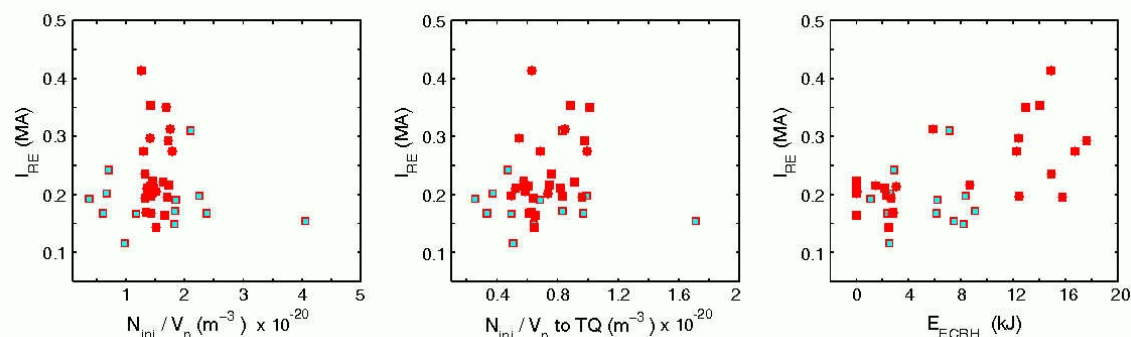

Figure 2. Measured RE current versus (left) the total amount of injected argon atoms per plasma volume, (centre) the amount of argon atoms injected per plasma volume during the pre-thermal quench phase and (right) the ECRH energy injected (and absorbed?) after the beginning of the pre-TQ. **Red** *data points have $N_{inj}/V_p = 1.5\times10^{20}$ +/- 20 % m^{-3}.*

Fig. 2 shows the value of the initial I_{RE} versus N_{inj}/V_p (*left*) and versus the amount of impurity atoms injected during the pre-thermal-quench phase, $N_{inj}(\Delta t_{pre-TQ})/V_p$ (*centre*) respectively. The pre-TQ phase lasts 2 – 4 ms while the valve reservoir is empty after ~ 10 ms. Although all data points have similar plasma equilibria and dimension, density and heating power, I_{RE} does not seem to scale with N_{inj}, which is the only variable which was scanned within a factor of 10.

An unexpected finding was the evidence that the ECRH power, inadvertently generated during the pre-TQ and fast CQ, can have an influence on I_{RE} (see fig. 2 *right*). This influence is difficult to understand because during the pre-TQ the injected gas creates a high density layer around the plasma, which reflects the injected power. A potential dependence of I_{RE} on the pre-TQ duration, on dI_p/dt, on Δl_i and ΔI_p at the TQ, and on equilibrium parameters was also checked but not found.

These experimental observations led to the use of the following 0-D fluid model to gain some understanding of the conversion of the poloidal magnetic flux into I_{RE}.

The I_{RE} is generated by the large electric field (E) associated with the fast I_p quench. The Dreicer and the secondary generation mechanisms are both responsible for the generation and are described by known first order differential equations, indicated shortly with $[dn_{RE}/dt]_1$ and $[dn_{RE}/dt]_2$ in this manuscript, and outlined in [4]. Loss mechanisms are not activated in the model; this corresponds to the experimental observation that the TQ, or phase of large magnetic perturbation, ends when the fast CQ starts. Therefore the following system of equations was explicitly integrated with a small time step:

$$E = -\frac{dI_p}{dt}\frac{L}{2\pi R_0} F_{mag}$$

$$E = \rho(j_p - j_{RE})$$

$$j_p = I_p/(\pi a^2 k)$$

$$j_{RE} = I_{RE}/(\pi a^2 k) = c e n_{RE}$$

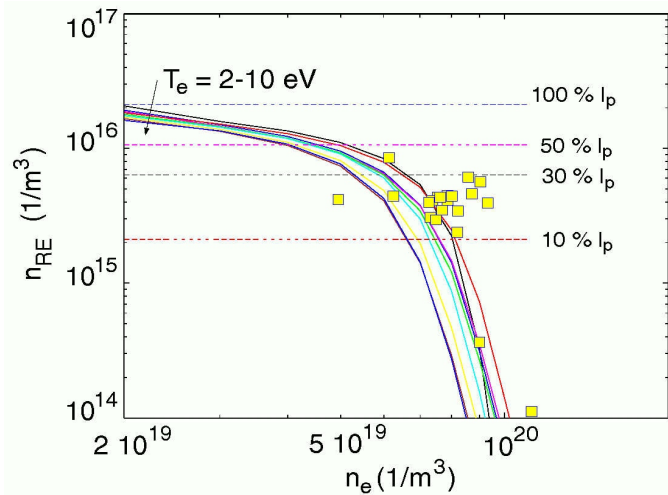$$\frac{dn_{RE}}{dt} = \left[\frac{dn_{RE}}{dt}\right]_1 + \left[\frac{dn_{RE}}{dt}\right]_2$$

Figure 3. RE current calculated with the 0-D model for several electron and argon density and temperature values (lines with different colors). The yellow data points represent experimental measurements.

The symbols in the equations, not yet introduced, have the following meanings: L is the total plasma self inductance, R_0 and "a" are the major and minor radius, F_{mag} is the fraction of poloidal magnetic energy dissipated or converted into RE in the plasma, k is the plasma elongation, ρ is the electrical resistivity, j_p and j_{RE} are the total and the RE current density, c is the light speed, e is the electron charge and n_{RE} is the RE particle density.

Fig. 3 shows the magnitude of I_{RE} expected by the 0-D model for the density range $n_e = 2\times10^{19} - 2\times10^{20}$ m^{-3} and $T_e = 2 - 10$ eV, for $I_p = 0.8$ A, a = 0.5 m, $R_0 = 1.68$ m respectively, internal inductance $l_i = 0.7$ and $F_{mag} = 0.8$. The Dreicer and secondary generation mechanisms are strong variables of n_e, T_e and of the effective ion charge, $Z_{eff} = 1 + Z_{Ar} n_{Ar}/n_e$. This last was calculated using tabulated values of $Z_{Ar}(T_e, n_e)$. The background deuterium density was kept fixed at 2×10^{19} m^{-3}.

For $n_e < 5 \times10^{19}$ m^{-3},the conversion of the thermal current into I_{RE} is predicted to be > 50 %. For $n_e > 5 \times10^{19}$ m^{-3}, I_{RE} is predicted to depend strongly on n_e and vanish for $n_e > 10^{20}$ m^{-3}. The experimental points (yellow squares) are superimposed to the 0-D results in fig. 3. The data points pertain to a subset of discharges resulting from the intersection of two sets: the set of shots with correct CO_2

interferometer measurements and a set of similar discharges. The measured I_{RE} is expressed as n_{RE} and the measured n_e (calculated as in fig.1) is used as a "proxy" for the RE beam density background. In fact, the n_e relevant to the RE generation cannot be measured. It is the density in the plasma core, where the RE are created, just after the TQ, during the $1 - 2$ ms of the fast CQ. It is not known how much of the argon, assimilated outside of the q=2 surface during the pre-TQ, is convected into the plasma during the TQ.

Given the large uncertainty affecting the density distribution, the experimental data points are consistent with the 0-D model. Several of them lie to the right of the calculated $n_{RE}(n_e)$ curves. This could indicate that the density measured by the interferometer is not uniformly distributed and still larger at the plasma edge than at the centre. In addition, the variability of Δt_{pre-TQ} and of F_{eff} among similar discharges can also influence the apparent lack of $I_{RE} - N_{inj}$ dependence.

Assuming an initial population of REs (seed) does not change considerably the result. It was verified that varying the equilibrium parameters within their measured variability ranges does not explain the observed scatter of the I_{RE} values in fig. 3.

The 0-D model can also be used to infer an average T_e during the fast CQ. The dI_p/dt calculated during the first ms of the fast CQ is plotted versus T_e in fig. 4 *left*. The experimental range of $dI_p/dt = 1.8 - 2.6$ 10^8 A/s corresponds, according to calculations, to $T_e = 3.5 - 7$ eV and $Z_{eff} = 1.7 - 2.7$, shown in fig. 4 *centre* and *right*. Appropriate spectroscopic measurements could confirm these values of T_e and Z_{eff}.
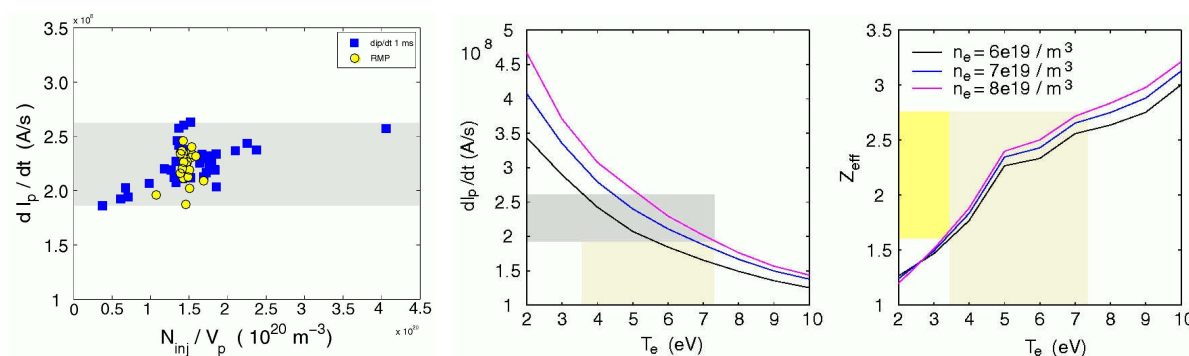

Figure 4. Left: Measured fast plasma current decay rate after TQ. Centre: calculated plasma current decay versus electron temperature. Right: calculated effective charge versus electron temperature.

Conclusions

The apparent discrepancy between the magnitude of RE current observed after argon-induced disruptions in AUG and the injected amount of argon has motivated (1) a careful analysis of the density measurements and (2) the calculation of the RE generation with a simple 0-D fluid model. Within the uncertainties affecting the density profile, experimental measurements fall in the ballpark of the predicted RE current magnitude. Nevertheless profile and kinetic effects should be studied to confirm this first result.

The RE current scatter, seen in the experiments, can only be partly attributed to measurable plasma or machine parameters; differences in the evolution of the MHD modes during the TQ could cause the random losses.

References
[1] MN Rosenbluth et al., 1997 Nuclear Fusion **37** 1355
[2] G Pautasso et al., 2017 Plasma Phys. Control. Fusion **59** 014046
[3] M Gobbin et al., 2018 Plasma Phys. Control. Fusion **60** 014036
[4] P. Helander et al., 2002 Plasma Phys. and Control. Fusion **44** B247